# Wave-based characterizations of soils derived from rock weathering

## Caractérisations des sols dérivés de la dégradation de roches par la méthode acoustique

Y. H. Wang
*The Hong University of Science and Technology, Hong Kong*
X. Dong
*Hangzhou Metro Group Co., LTD, China*

ABSTRACT

This paper reports wave-based characterizations of soils derived from rock weathering. Results from testing two commonly encountered saprolitic soils in Hong Kong and residual soils in Puerto Rico (from previously published data) reveal the features of soil behavior in response to bonding effects, yielding, and the influences of weathering. The features were captured in the α factor and β exponent of the velocity ($V_s$)-stress($\sigma'$) relationship, $V_s = \alpha(\sigma'/1kPa)^{\beta}$. When bonding effects prevail, including capillary suction and precipitated fines or salts around contacts under unsaturated conditions, a higher α value and a lower β exponent can be measured, i.e., the soil structure is stiffer and less sensitive to changes in the stress state. Saturation destroys those apparent bonds, which in turn weakens the soil skeleton and increases the compressibility. Thus, a lower α factor and a higher β exponent are found. A decreasing and increasing trend can be observed for the α and β coefficients during soil yielding because this process moves towards restructuring the soil skeletons accompanied by higher compressibility. Weathering effects lead to a decreasing trend in α values, suggesting that a looser packing or a more opened structure and softer particles (e.g., more fines contents) are formed in response to higher degrees of weathering. The tendency of weathering in producing greater fines contents and opened/weaker soil skeletons eventually leads to a higher damping ratio, $D_{min}$, in soils.

RÉSUMÉ

Cet article présente les caractérisations des sols dérivés de la dégradation de roches obtenues à partir de la méthode acoustique. Les résultats des analyses de deux sols saprolitiques à Hong Kong et de sols résiduels à Porto Rico (des données précédemment publiées) donnent les caractéristiques du comportement de sols en réponse aux effets de la cimentation, de la plastification et de la dégradation. Les caractéristiques ont été déterminées en introduisant deux paramètres α et β rendant compte de la relation entre la vitesse et la contrainte, $V_s = \alpha(\sigma'/1kPa)^{\beta}$. Lorsque les effets de cimentation prédominent, comprenant la succion capillaire et les fines ou les sels précipités autour des contacts dans des conditions non-saturées, une valeur plus élevée de α et une valeur moins élevée de β peuvent être mesurées, c'est à dire que la structure du sol est plus rigide et moins sensible aux changements de l'état de contrainte. La saturation détruit ces cimentations apparentes, ce qui conduit à affaiblir le squelette du sol et à augmenter sa compressibilité. Ainsi, une valeur moins élevée de α et une valeur plus élevée de β sont obtenues. On peut observer une tendance à la diminution pour le paramètre α et une tendance à l'augmentation pour le paramètre β pendant la plastification du sol parce que ce processus induit une restructuration des sols accompagnée d'une compressibilité plus élevée. Les effets de la dégradation conduisent à une tendance à la diminution de α. Cela montre qu'un emballage plus lâche ou une structure plus ouverte et des particules plus molles (par exemple, plus de fines) sont formés lorsque le degré de dégradation est plus élevé. La dégradation produisant une plus grande proportion de fines et des squelettes de sol plus ouverts/faibles conduit à un rapport d'amortissement plus élevée, $D_{min}$, pour les sols.

Keywords: velocity-stress relationship; damping ratio, saprolites, weathering effect.

## 1 INTRODUCTION

Residual and saprolitic soils are derived from in-situ rock decomposition. Thus, the engineering properties highly rely on the weathering environment such as features of the parent rocks, the climate, the topography, and drainage conditions (e.g., Vaughan 1988). Such localized and unique formation histories lead to soil behavior varying from places to places. Volcanic tuffs and granites are the two most abundant rocks in Hong Kong and cover about 65% and 28% of the land area, respectively (Shaw 1997). The unavoidable physical and chemical weathering processes gradually alter the ground profiles from rocks to soils (e.g., see Irfan 1996 and 1999). Hence, most of the construction projects in Hong Kong have to consider these particular soils from rock weathering, and the need to have better understandings on these soils is evident. The wave-based characterization provides an effective means to gain insights into soil behavior in various aspects and therefore can fulfill such a need. In this study, the wave-based measurement is conducted to reexamine the behavior of these particular soils under the influence of bonding, yielding, and different weathering degrees, with particular emphasis on the contact behavior between particles.

## 2 REVIEW OF THE PARAMETERS USED IN WAVE-BASED CHARACTERIZATIONS

The shear wave velocity, $V_s$, and associated damping ratio, $D$, (the S-wave mode) are the two parameters used in wave-based characterizations. The wave sent into the soils has a strain level less than the linear threshold strain, $\gamma_{tl}$, ~$10^{-5}$. Thus, the S-wave velocity, $V_s$, is associated with the maximum shear modulus, $G_{max}$, and the damping ratio is the minimum damping ratio, $D_{min}$.

### 2.1 *Velocity-stress relationships and associated contact behavior of soils*

Experimental results indicate that the S-wave velocity depends on the stresses in the directions of wave propagation ($v$) and polarization ($h$) (Roesler 1979). An empirical relation is introduced to describe this dependence:



*doi:10.3233/978-1-60750-031-5-380*

$$V_s = \alpha\left(\frac{\sigma_v'}{1kPa}\right)^{\theta}\left(\frac{\sigma_h'}{1kPa}\right)^{\delta} \quad (1)$$

where $\theta$, $\delta$, and $\alpha$ are experimentally determined parameters. The experimental observations also suggest that Eq. (1) can be modified in terms of the average stress within the pane of wave travel (Yu and Richart 1984):

$$V_s = \alpha_1\left(\frac{\sigma_v' + \sigma_h'}{2kPa}\right)^{\beta} \quad (2)$$

where $\beta$ is equal to $\theta + \delta$ but the alpha factor is different with that in Eq. (1). Under an isotropic stress condition $\sigma_0'$, the above two equations become the same:

$$V_s = \alpha\left(\frac{\sigma_0'}{1kPa}\right)^{\beta} \quad (3)$$

In the $K_0$-stress condition, $\sigma_v' = K_0\sigma_h'$, very often only $\sigma_v'$ is known. Eqs. (1) and (2) are therefore rewritten as,

$$V_s = \alpha K_0^{\delta}\left(\frac{\sigma_v'}{1kPa}\right)^{\theta}, \text{ and} \quad (4)$$

$$V_s = \alpha_1\left(\frac{1+K_0}{2}\right)\left(\frac{\sigma_v'}{1kPa}\right)^{\beta}, \text{ or simply as} \quad (5)$$

$$V_s = \alpha_2\left(\frac{\sigma_v'}{1kPa}\right)^{\beta} \quad (6)$$

where $K_0$ is the earth pressure coefficient at rest. The alpha factor now includes the $K_0$ coefficient. If the $K_0$ coefficient is not a constant and is stress dependent, the beta exponent is also changed with the $K_0$ value.

The above empirical velocity-stress relationships gain support by comparing with the analytic solution based on the Hertzian-Mindlin contact for the case: isotropic loading on a statically isotropic packing with constant fabrics (Chang et al. 1991),

$$V_s = \rho^{-\frac{1}{2}}G_g^{1/3}\left(\frac{5-4\nu_g}{5(2-\nu_g)}\right)^{\frac{1}{2}}\left[\frac{\sqrt{3}cn}{\sqrt{2}(1-\nu_g)(1+e)}\right]^{\frac{1}{3}}\sigma_0'^{1/6} = \alpha_3\left(\frac{\sigma_0'}{1kPa}\right)^{1/6} \quad (7)$$

where $cn$ is the coordination number, $\nu_g$ and $G_g$ are respectively the Poisson's ratio and shear modulus of the materials that make the particle, $\sigma_0'$ is the isotropic confinement, $\rho$ is the density of packing, and $e$ is the void ratio. Comparing this equation with the empirical relations, e.g., Eq. (3), reveals that the contact behavior can be reflected in the beta exponent. For instance, 1/6 is for the Hertzian contact and 0 for a perfect solid. The alpha factor varies with the packing characteristics (i.e., $cn$, $e$, and $\rho$) and the material properties of the particles (i.e., $\nu_g$ and $G_g$) (Santamarina et al. 2001). A denser/stronger packing and stiffer particle can give rise to a higher alpha value. Nevertheless, it should be noted that the constant-fabric assumption for Eq. (7) is not applicable to most of the measurements. In order to establish the velocity-stress relationship, the applied stress has to be changed in the measurement as does the soil fabric. Hence, the experimentally determined beta exponent not only captures the contact behavior of soils but also the effect of fabric changes (Santamarina et al. 2001). For instance, if alterations of the soil fabric are severe in response to the change of stress states, e.g., the case of normally consolidated clays, the beta exponent will be higher to accommodate the associated effects.

Although the alpha and beta parameters are implicitly determined by different interrelated soil properties, a general trend between the two parameters for different types of soils under isotropic confinement can still be found (see Fig. 1). The trend exhibits similar soil behavior as discussed above. The normally consolidated (NC) clay exhibits a lower value of α and a higher β exponent because of its weaker structure and higher compressibility during loading. Due to a denser/stronger structure and fewer fabric changes to loading in overconsolidated (OC) clays, a greater α factor and smaller β exponent is found. Cemented soils have a higher α factor and a lower β exponent as long as the cementation effects still overwhelm the influence from the state of stress. Collectively, soils with stiffer particles and stronger/denser packing will exhibit a higher α vale and a lower β exponent. Bonding effects and the associated features of structured soils are important characteristics for soils derived from rock weathering (e.g., see Vaughan 1988). Thus, their velocity-stress relationships should demonstrate a higher α value and a lower β exponent. Moreover, it is expected that the higher the degree of weathering, the lower the value of α and the higher the β exponent (to be discussed in detail later).

### 2.2 *Damping ratio $D_{min}$ and its relevance to soil types and weathering effects*

The $D_{min}$ of saturated clays is about 1.4% ~ 5%, which is much higher than the value of dry or saturated sands ($D_{min}$ = 0.2% ~ 0.8%). Lanzo and Vucetic (1999), based on the published trend, also suggested that $D_{min}$ increases with the plasticity index PI. These observations can be attributed to that clay has a greater energy loss of a viscous type, including the squirting flow between particle contacts. The damping ratio is a ratio between the energy loss and the energy stored; the latter one is proportional to the associated shear modulus. Therefore, under the same amount of energy loss, if a soil has a weaker structure, i.e., a lower stiffness, the associated damping ratio should be smaller. Weathering tends to produce higher fines contents (i.e., more clay content) and more opened/weaker structures (i.e., a lower soil stiffness). These features are expected to lead to a higher damping ratio, $D_{min}$.

## 3 EXPERIMENTAL INVESTIGATIONS

### 3.1 *Descriptions of two commonly encountered saprolitic soils in Hong Kong*

Two commonly encountered saprolitic soils in Hong Kong are mainly concerned in this paper, called weathered volcanic tuff (WT) and weathered granite (WG) here. The WT samples were taken from a housing development site located in Fei Ngo Shan, Sai Kung while the WG samples were taken from a slope in Butterfly Valley, Sha Tin. Both soils were unsaturated in their in-situ states. Large block samples, ranging from a minimum of 250 mm to a maximum of 400 mm cubes, were extracted from the ground by hand-held equipment in order to minimize sampling disturbance and preserve the original soil structure. The sampling level for WT ranged from 3 m to 5 m below the existing ground level, while WG was taken from about 1.5 m below the existing slope surface. The samples were then placed inside sealed boxes and stored in a moisture-controlled room before being trimmed into properly sized specimens for tests. Relict joints or fissures were readily seen in WT but were not

apparently visible in WG. The particle size distributions show that both WT and WG are well graded. In addition, WT mainly consists of silt-sized particles (~70%), and WG contains coarser particles and more clay-sized materials (~27%).

### 3.2 *Experimental details*

A modified oedometer cell with a height of 50 mm and a diameter of 70 mm were used in the test. A bender element set was installed in the top and bottom caps of the cell to measure the S-wave velocity under the $K_0$-stress condition. The cell height was a compromise between minimizing the side friction from the cell walls, and reducing the error percentage occurring in determining the arrival time. The S-wave emitted by the bender element propagates along the vertical loading direction ($v$) and polarizes in the horizontal direction ($h$). The intact WT and WG specimens were carefully trimmed from the block sample to preserve the soil's structure. Saturation of the specimen was made by flushing the $CO_2$, followed by de-aired water (a vacuum pressure of 20 kPa was applied at this stage). Each loading stage was lasted for 24 hours during consolidation; the completeness of the primary consolidation was also assessed by the converging trend of measured S-wave velocity with time elapsed. The inner surface of the cell wall was smeared with silicone grease during testing to minimize the side friction. The measurement of $D_{min}$ was conducted using resonant column testing under the saturated condition. The applied confining pressure is from 50 kPa to 250 kPa in the test.

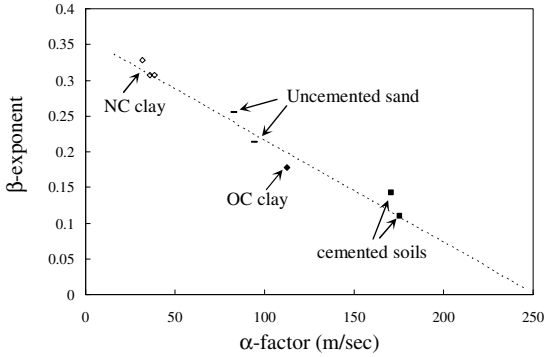


Figure 1. Typical values for α and β coefficients of the velocity-stress relationships, i.e., Eq. (3) (based on Santamarina et al. 2001). Some of the data are compiled from Baig et al. (1997), Fratta and Santamarina (2002), and the author's study.

## 4 RESULTS AND DISCUSSIONS

Fig. 2 shows the results of WG specimens subjected to $K_0$-loading under in-situ water content of $w$ = 12.8% (unsaturated) and saturated conditions. As shown in Fig. 2-a, the yield exhibits a gradual change and is not as distinct as that occurring in the soils with a higher void ratio, e.g., see results in Wesley (1974). The initial void ratio of the unsaturated WG specimens is about 0.62. By simply extending the two straight line portions, the quasi-preconsolidation stress or yield stress can be identified in a subjective manner, which is about 135 kPa and 316 kPa for the saturated and unsaturated cases, respectively. The evolution of S-wave velocities is presented in Fig. 2-b. In both saturated and unsaturated WG specimens, a faster velocity is detected during unloading instead of loading because the densification effects overwhelm the influence from the bonding breakages. In Fig. 2-a, larger vertical strains are measured especially under the saturated condition. This can be attributed to the fact that the WG specimen consists of higher clay contents (clay-sized particles are ~27%). Such a deformation tendency leads to the result: the S-wave velocity of the saturated specimen finally is higher than that for the unsaturated specimen when the vertical effective stress is greater than ~558 kPa (Fig. 2-b).

The semi-log plot, Fig. 2-c, showing only the behavior during loading, suggests that yields and the associated variations of the velocity-stress relationship occur over a transition range rather than at a distinct point. This reflects the observation of the stress-strain response (Fig. 2-a). In order to capture such a transition process, curve fitting by different velocity-stress relationships (using Eq. (6)) within a proper stress range is adopted; for completeness, the coefficient of determination, $R^2$, is also indicated in the figure. Based on the above discussions of the α and β coefficients, salient findings in Fig. 2-c are summarized as follows. Note that similar observations also can be found in the WT specimens (the results are not shown here because of the limited space).

(1) A decreasing and increasing trend can be respectively observed in the α and β coefficients during the gradual yield because this process moves towards restructuring the soil skeletons accompanied by higher compressibility/severe fabric alterations. This fact also implies that the α and β coefficients are varied before and after yielding. Thus, the stress range used to derive the velocity-stress relationships should be specified whether it is greater or less than the yield stress.

(2) For the unsaturated specimen, the bonding effects arising from capillary forces and precipitated fines or salts around the contacts are appreciable. These apparent bonds give rise to a higher value of α and a lower β exponent. Saturation destroys such bonding, which in turn weakens the structure and increases the compressibility. This results in a lower α factor and a higher β exponent.

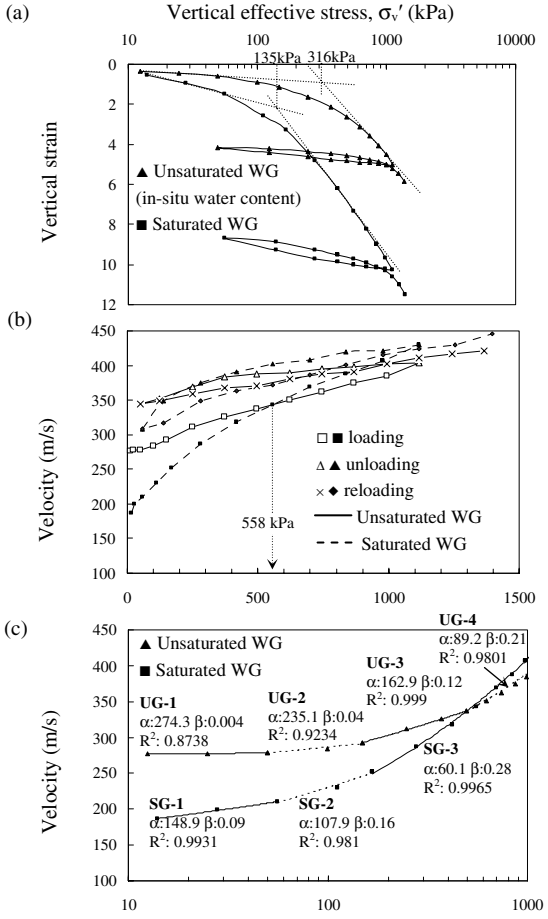


Figure 2. Results of the saturated and unsaturated WG specimens: (a) vertical strain versus vertical stress, (b) velocity versus vertical stress, and (c) velocity versus vertical stress (semi-log scale).

The measured damping ratios, $D_{min}$, of the WG and WT samples under the saturated condition are about 2.5% and 1.5%, respectively. The associated shear modulus of the WG sample is greater than that of the WT sample. Thus, the higher $D_{min}$

measured in WG sample is mainly attributed to its higher clay/fines contents.

## 5 A REEXAMINATION OF PREVIOUSLY PUBLISHED RESULTS *ON RESIDUAL SOILS*

Weathering processes tend to produce a weaker and more opened soil structure with greater fines or clay contents. Furthermore, these features are expected to be more distinct for soils at shallower depths because the weathering degree increases with decreasing depth. As shown in Fig. 3-a, the previously published data on the basaltic residual soils in Puerto Rico demonstrate these characteristics. These features also result in the damping ratios ($D_{min}$) increasing with weathering grades as presented in Fig. 3-b.

As shown in Fig. 3-a, weathering effects can also be reflected in the α factor and β exponent of the velocity-stress relationships (using Eq. (3)). The decreasing trend in α values suggests that looser packing (e.g., a more opened structure and fewer coordination numbers) and softer particles (e.g., more fines contents) are formed in response to weathering. The rising trend of β exponents can be explained as follows. The isotropic confinement adopted to derive the velocity-stress relationship ranges from 34.5 kPa to 275.8 kPa (5 psi to 40 psi), which is greater than the yield stress based on the results of one-dimensional consolidation. Thus, appreciable settlement accompanied by severe fabric changes will occur, especially in the soils with higher weathering grades due to more opened and weaker structures. As a result, the β exponent increases with an increase in weathering grades. Compared with other types of soils (as those shown in Fig. 1), these basaltic residual soils behave like uncemented sand but less stiff (smaller α values) after yielding. The bonding effects are not distinct because the applied stress has already made soil yield.

## 6 CONCLUSIONS

In this paper, wave-based characterizations are applied to gain insights into the behavior of soils derived from rock weathering, including the effects of bonding, yielding, and weathering.

The bonding effects and yielding processes can be captured in the α factor and β exponent of the velocity-stress relationship. While the bonding effects prevail, a higher α value and a lower β exponent are measured, i.e., the soil structure is stiffer and less sensitive to changes in the stress state. Under the unsaturated condition, capillary forces and precipitated fines or salts around contacts can render appreciable bonding effects. Thus, a higher value of α and a lower β exponent are shown. On the other hand, saturation destroys such bonding, which in turn weakens the soil structure and increases the compressibility. This results in a lower α factor and a higher β exponent. A decreasing and increasing trend can be found for the α and β coefficients, respectively, during soil yielding because this process moves towards restructuring the soil skeletons accompanied by higher compressibility. The α and β coefficients are varied before and after yielding so that the stress range used to derive the velocity-stress relationships should be specified whether it is greater or less than the yield stress.

Weathering effects are associated with the α and β coefficients. The decreasing trend of α values suggests that looser packing or a more opened structure and softer particles (e.g., more fines contents) are formed in response to weathering. The trend of the β exponent depends on the magnitude of the applied stress, i.e., greater or less than the yield stress, and the saturation condition. If the stress applied is over the yield stress, appreciable settlement accompanied by severe fabric alterations will occur, especially in soils with higher weathering grades due to more opened and weaker structures. As a result, the β exponent increases with an increase in weathering grades. The weathering tendency towards producing greater fines contents and opened/weaker structures can lead to a higher damping ratio, $D_{min}$, of soils.

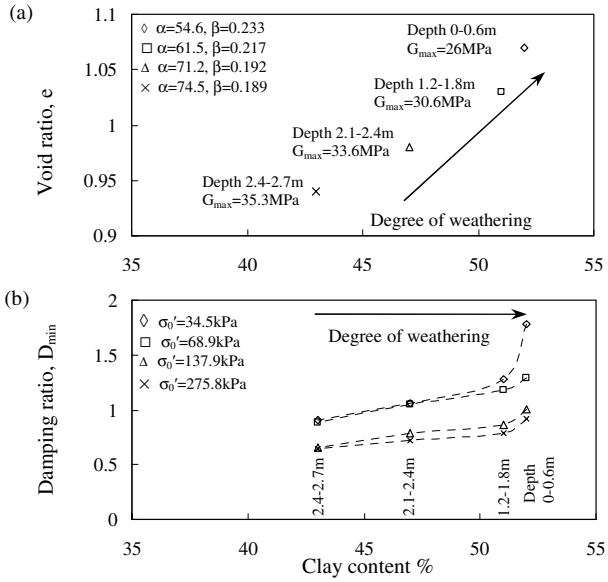


Figure 3. Characteristics of basaltic residual soils in Puerto Rico: (a) void ratio, modulus, and clay content versus sampling depth (the maximum shear modulus $G_{max}$ is measured under the confining pressure $\sigma_0'$=34.5 kPa) and (b) degree of weathering and clay content versus damping ratio $D_{min}$. (data from Macari and Hoyos 1996).

## ACKNOWLEDGEMENT

This research was supported by the Research Grants Council, Hong Kong and the Hong Kong University of Science and Technology.

## REFERENCES

Baig, S., Picornell, M. & Nazarian, S. 1997. Low strain shear moduli of cemented sands. *Journal of Geotechnical and Geoenvironmental Engineering* 123(6): 540-545.

Chang, T.S., Misra, A. and Sundaram, S.S. (1990), "Properties of granular packings under low amplitude cyclic loading, *Soil Dynamics and Earthquake Engineering*, Vol. 10, pp. 201-211.

Fratta, D. & Santamarina, J.C. 2002. Shear wave propagation in joined rock: state of stress. *Géotechnique* 52(7): 495-505.

Irfan, T.Y. 1996. Mineralogy, fabric properties and classification of weathered granites in Hong Kong. *Quarterly Journal of Engineering Geology* 29: 5-35.

Irfan, T.Y. 1999. Characterization of weathered volcanic rocks in Hong Kong. *Quarterly* Journal *of Engineering Geology* 32: 317-348.

Lanzo, G. & Vucetic, M. 1999. Effect of soil plasticity on damping ratio at small cyclic strains. *Soils and Foundations* 39(4): 131-141.

Macari, E.J. & Hoyos Jr. L. 1996. Effect of degree of weathering on dynamic properties of residual soils. *Journal of Geotechnical and Geoenvironmental Engineering* 122(12): 988-997.

Roesler, S.K. 1979. Anisotropic shear modulus due to stress anisotropy. *Journal of Geotechnical Engineering, ASCE* 105: 871-880.

Santamarina, J. C., Klein, K. A., & Fam, M. A. 2001. *Soils and Waves*. John Wiley & Sons, LTD. New York.

Shaw, R. 1997. Variations in sub-tropical deep weathering profiles over the Kowloon granite, Hong Kong. *J. Geological Society* 154: 1077-1085.

Vaughan, P.R. 1988. Characterizing the mechanical properties of in situ residual soil. In *Proceedings of the 2nd International Conference on Geomechanics in Tropical Soils*, Singapore, Vol. 2, pp. 469-487.

Wesley, L. D. (1974). Discussion on "Structural behavior of residual soils of the continually wet highlands of Papua New Guinea". *Géotechnique* 24(1): 101-105.

Yu, P. & Richart, F.E. Jr. 1984. Stress ratio effects on shear modulus of dry sands. *Journal of Geotechnical Engineering, ASCE* 110(3): 331-345.